



On the modelling of wave breaking and set-up on coral reefs

S.R. Massel^{a,*}, M.R. Gourlay^b

^a *Australian Institute of Marine Science, Townsville, Qld 4810, Australia*

^b *Department of Civil Engineering, The University of Queensland, Brisbane, Qld 4072, Australia*

Received 24 March 1999; received in revised form 9 August 1999; accepted 30 August 1999

Abstract

An extended refraction–diffraction equation [Massel, S.R., 1993. Extended refraction–diffraction equation for surface waves. *Coastal Eng.* 19, 97–126] has been applied to predict wave transformation and breaking as well as wave-induced set-up on two-dimensional reef profiles of various shapes. A free empirical coefficient α in a formula for the average rate of energy dissipation $\langle \epsilon_b \rangle = (\alpha \rho g \omega / 8\pi)(\sqrt{gh} / C)(H^3 / h)$ in the modified periodic bore model was found to be a function of the dimensionless parameter $F_{c0} = (g^{1.25} H_0^{0.5} T^{2.5}) / h_r^{1.75}$, proposed by Gourlay [Gourlay, M.R., 1994. Wave transformation on a coral reef. *Coastal Eng.* 23, 17–42]. The applicability of the developed model has been demonstrated for reefs of various shapes subjected to various incident wave conditions. Assuming proposed relationships of the coefficient α and F_{c0} , the model provides results on wave height attenuation and set-up elevation which compare well with experimental data. © 2000 Elsevier Science B.V. All rights reserved.

Keywords: Marine environment; Coral reefs; Mathematical methods; Measurements; Surface waves

1. Introduction

Coral reefs occur in the tropical regions of the Pacific, Indian and Atlantic Oceans in the form of fringing reefs surrounding islands, barrier reefs or separate atolls and island reefs (Veron, 1986). Increased economic pressure for development, increased impact from land-based and marine industries, and increased access to coral reef areas have all

* Corresponding author. Institute of Hydroengineering, ul. Kościarska 7, 80-953 Gdansk, Poland. Tel.: +48-552-20-11; fax: +48-552-42-11; e-mail: smas@ibwpan.gda.pl

lead to the demands to provide a sound engineering and environmental basis for infrastructure developments in reefal areas. This can only be achieved through comprehensive understanding of the physical processes which shape the reef environment and control its ecology. Wave action is a significant contributor to these processes. Energy of waves propagating over the reef slope and water turbulence associated with wave breaking impose forces on the various types of structures located on the reef. Moreover, water movement is essential for reef zonation and segregation of organisms.

Owing to steep slopes, large roughness of the reef bottom and complicated bottom slope, coral reef hydrodynamics presents considerable difficulties for both experiments and numerical modelling. Therefore, experimental and theoretical papers on waves on reefs are not numerous. Gourlay (1994; 1996a; b; 1997) in a series of papers reported the results of very comprehensive laboratory studies on reef hydrodynamics. These results will be used extensively in this paper.

Field measurements of waves breaking on a reef and propagating into a lagoon were obtained by Lee and Black (1979), Gerritsen (1981), Roberts (1981), Young (1989) Hardy and Young (1996), Hardy et al. (1991), and Massel and Brinkman (1998).

Theoretical descriptions and numerical models of reefs are even rarer. Gerritsen (1981) presented a very comprehensive report on measurement and calculation of wave parameters on reefs. However, his approach was based mostly on the hydraulics' type of analysis rather than on the solution of the corresponding boundary value problem. Massel (1993) developed an extended refraction–diffraction equation which allows substantial variations in water depth and arbitrary bottom curvature. This equation was subsequently supplemented by the dissipation term providing an analytical tool for modelling of waves which propagate over a reef and break (Massel, 1996a). However, in this model, a free empirical coefficient α describing the intensity of wave breaking must be assumed a priori or known from experiments.

This paper is aimed at the development of a predictive type model for wave propagation and breaking over an arbitrary reef slope. The statement “predictive” means that the intensity of breaking is estimated using the initial deepwater wave parameters and reef geometry. In the proposed model, a system of equations for wave height and wave-induced set-up is solved simultaneously in an iterative manner. The data from laboratory experiments by Gourlay (1994; 1996a; b) have been used to calibrate a free empirical coefficient of the model. Examples of the application of the developed approach for various reef types, in the laboratory as well as in natural scales, are given.

2. Numerical model

2.1. Velocity potential in particular regions of wave motion

Consider the coordinate system $O(x, y, z)$ with z -axis positive upwards and equal to zero at the still water level, the x -axis directed perpendicularly to the reef and the y -axis extending alongshore (Fig. 1). The transect in Fig. 1a illustrates a typical cross-section

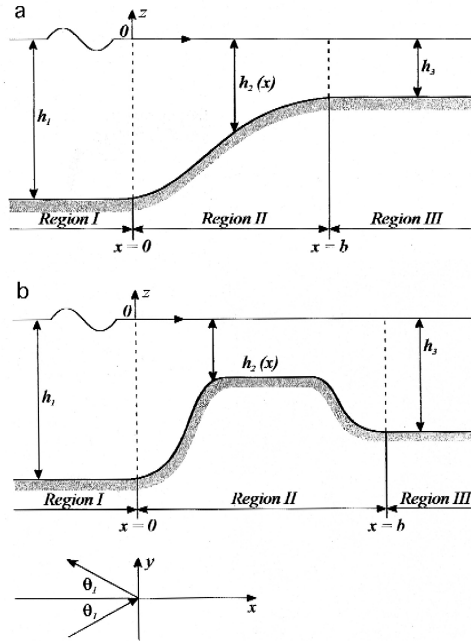


Fig. 1. Reef types: (a) fringing reef, (b) platform reef.

through a fringing reef, while in Fig. 1b the cross-section for platform reef is shown. Both reefs are assumed to be elongated along the y -axis. To facilitate a numerical analysis, the whole area of interest was divided into different regions in which governing equations are established. The solutions in particular regions are matched using appropriate conditions for continuity of pressure and velocities. In Region II: $0 \leq x \leq b$, $-\infty < y < \infty$, the water depth $h(x)$ is a varying function of x . In Region I ($x \leq 0$) and Region III ($x \geq b$), the water depth is constant and equal to h_1 and h_3 , respectively. A plane regular wave arrives at an angle Θ_1 with respect to the x -axis. The incident wave height is equal to H_i and the wave frequency is equal to ω . The value of incident wave height H_i is determined from a deepwater wave height H_0 , water depth h and wave frequency ω using the linear wave theory.

In Region I, the wave field consists of incident and reflected waves, and potential Φ_1 takes the form (Massel, 1993):

$$\Phi_1(x, y, z, t) = \frac{-igH_i}{2\omega} Z_1(z) [\exp(ik_1 x \cos \Theta_1) + K_R \exp(-ik_1 x \cos \Theta_1)] \times \exp(i\chi y) \exp(-i\omega t), \quad (1)$$

in which:

$$Z_1(z) = \frac{\cosh k_1(z + h_1)}{\cosh k_1 h_1}, \quad (2)$$

$$\chi = k_1 \sin \Theta_1; \quad (3)$$

the K_R is an unknown complex reflection coefficient and wave number k_1 should satisfy the dispersion relation:

$$\omega^2 = gk_1 \tanh(k_1 h_1). \quad (4)$$

Under the assumption that there are no reflected waves in the Region III, the potential in this Region represents only progressive waves propagating in the direction of the positive x -axis, i.e.:

$$\Phi_3(x, y, z, t) = \frac{-igH_1}{2\omega} Z_3(z) K_T \exp(ik_3 x \cos \Theta_3) \exp(i\chi y) \exp(-i\omega t), \quad (5)$$

in which:

$$Z_3(z) = \frac{\cosh k_3(z + h_3)}{\cosh k_3 h_3}, \quad (6)$$

the K_T is an unknown complex coefficient, and wave number k_3 and angle Θ_3 should satisfy the dispersion relation:

$$\omega^2 = gk_3 \tanh(k_3 h_3) \quad (7)$$

and Snell's law (Massel, 1989):

$$\chi = k_1 \sin \Theta_1 = k_3 \sin \Theta_3. \quad (8)$$

In Region II, water depth $h(x)$ varies substantially and refraction and diffraction effects cannot be neglected. In order to account for these effects in this paper an approach based on the mild-slope equation (Berkhoff, 1973) is used. Massel (1993; 1996a), using the Galerkin-Eigenfunction method, extended the applicability of the mild-slope equation for steep slopes. The resulting refraction–diffraction equation includes the higher order terms and evanescent modes as well as the energy dissipation due to breaking and bottom friction. Thus, relatively rapid and physically realistic undulations in water depth at the coral reef can be handled. The governing velocity potential $\Phi(x, y, z, t)$ can be represented in the form (Massel, 1993):

$$\Phi_2(x, y, z, t) = \frac{-igH_1}{2\omega} Z_2(z) \varphi(x) \exp(i\chi y) \exp(-i\omega t), \quad (9)$$

in which:

$$Z_2(z) = \frac{\cosh k_2(z + h_2)}{\cosh k_2 h_2} \quad (10)$$

and

$$\frac{d^2\varphi}{dx^2} + (CC_g)^{-1} \frac{dCC_g}{dx} \frac{d\varphi}{dx} + [k_2^2(1 + \psi) + i\gamma k_2 - \chi^2] \varphi = 0, \quad (11)$$

where evanescent modes have been neglected. The $\varphi(x)$ is the non-dimensional wave height $H(x)/H_1$, C and C_g are the phase and group velocities, respectively, and wave number k_2 satisfies the dispersion relation:

$$\omega^2 = gk_2 \tanh(k_2 h_2). \quad (12)$$

The term ψ represents the influence of bottom slope and bottom curvature, i.e.:

$$\psi = E_1(k_2 h_2) \left(\frac{dh_2}{dx} \right)^2 + E_2(k_2 h_2) \frac{d^2 h_2}{dx^2} \quad (13)$$

in which $E_1(k_2 h_2)$ and $E_2(k_2 h_2)$ are complicated functions of $(k_2 h_2)$ and can be found elsewhere (Massel, 1994, 1996a). The damping factor γ is still unknown and will be determined later.

The potentials Φ_1 , Φ_2 and Φ_3 must satisfy the matching conditions which provide continuity of pressure and horizontal velocity, normal to the vertical planes separating the fluid regions. A general evaluation of these boundary conditions for arbitrary bottom slopes at $x = 0$ and $x = b$, using the orthogonality of functions Z , is given in another paper (Massel, 1993).

When the bottom profile $h_2(x)$ is arbitrary, a resulting boundary value problem can be solved only numerically. In this paper, a finite difference method has been used and the resulting system of linear equations for φ was solved by the Cholesky's method for a band type matrix (Haggerty, 1971).

2.2. Wave induced set-up and set-down

The shoaling, refraction, diffraction and dissipation processes induce the spatial changes in the radiation stress resulting in changes of mean sea level (MSL). Longuet-Higgins and Stewart (1964) have shown that a balance of sea level gradient and the gradient of radiation stress takes the form:

$$\frac{dS_{xx}}{dx} + \rho g (h + \bar{\eta}) \frac{d\bar{\eta}}{dx} = 0, \quad (14)$$

in which $\bar{\eta}$ is a change of MSL (wave set-up or set-down) due to wave action, and S_{xx} is a radiation stress tensor component. In Eq. (14), the resultant shear stress and oscillating part of the set-up have been neglected. The influence of these factors on a value of resultant set-up will be discussed in another paper. Using the representation (9) for velocity potential for substantially varying water depth, the radiation stress tensor S_{xx} can be written as follows (Dingemans, 1997):

$$S_{xx} = \frac{\rho g H_i^2}{16 \omega} \left\{ 2 C C_g \frac{\partial \varphi}{\partial x} \frac{\partial \varphi^*}{\partial x} + \omega^2 \left(\frac{2 C_g}{C} - 1 \right) \varphi \varphi^* + \frac{1}{2} (gh - C C_g) \frac{\partial^2 (\varphi \varphi^*)}{\partial x^2} \right\}, \quad (15)$$

in which the asterisk (*) denotes the complex conjugate value. Eq. (15) is valid for an arbitrary linear wave field, not only for purely progressive waves. However, as will be shown later, due to wave breaking, the reflection from the reef is rather small. Hence, if we neglect the reflected waves and introduce the wave energy E for progressive waves, the tensor S_{xx} takes a much simpler form (Massel, 1989):

$$S_{xx} = E \left(\frac{3}{2} m - \frac{1}{2} \right) + \frac{1}{2} E m \cos \Theta, \quad (16)$$

where:

$$E = \frac{1}{8} \rho g H^2 \quad (17)$$

$$H(x) = H_i \sqrt{[\Re \varphi(x)]^2 + [\Im \varphi(x)]^2}, \quad (18)$$

$$m = \frac{1}{2} \left(1 + \frac{2kh}{\sin 2kh} \right), \quad (19)$$

in which \Re and \Im are the real and imaginary parts of the complex function φ .

Owing to the rapidly changing water depth, the resulting gradient of the radiation stress is affected by the local gradients of wave height, wave number and wave direction, i.e.:

$$\frac{dS_{xx}}{dx} = \frac{1}{8} \rho g R(x), \quad (20)$$

in which:

$$R(x) = \left\{ \frac{\partial S_{xx}}{\partial H} \frac{dH}{dx} + \frac{\partial S_{xx}}{\partial m} \frac{dm}{dx} + \frac{\partial S_{xx}}{\partial \Theta} \frac{d\Theta}{dx} \right\}. \quad (21)$$

After substituting Eq. (20) into Eq. (14) we obtain:

$$\frac{d\bar{\eta}}{dx} = \frac{-1}{8(h + \bar{\eta})} R(x). \quad (22)$$

Eqs. (11) and (22) form a final set of equations for unknown non-dimensional wave height φ and set-up $\bar{\eta}$. This set of equations is solved in a recurrent manner, i.e., first a non-dimensional wave height φ is determined for $\bar{\eta} = 0$, then the set-up $\bar{\eta}$ is established and a new water depth ($h + \bar{\eta}$) is used in calculation of a new φ value. The process is repeated until the required accuracy is obtained. In this paper, Cholesky's method has been used for solving Eq. (11) and a predictor–corrector method was applied for Eq. (22).

2.3. Energy dissipation due to wave breaking

At steep coral reefs, two basic energy dissipation mechanisms dominate, i.e., dissipation due to wave breaking and due to bottom friction. Therefore, the total damping factor γ can be presented as (Massel, 1996a):

$$\gamma = \gamma_b + \gamma_f, \quad (23)$$

in which:

$$\gamma_b = \frac{8\langle \epsilon_b \rangle}{\rho g C_g H^2}, \quad (24)$$

$$\gamma_f = \frac{8\langle \epsilon_f \rangle}{\rho g C_g H^2}, \quad (25)$$

where $\langle \epsilon_b \rangle$ and $\langle \epsilon_f \rangle$ represent the average rate of energy dissipation (per unit area) due to wave breaking and bottom friction, respectively.

Wave breaking is a highly non-linear process and at present there is no theoretical solution to this problem. However, there is a wide body of literature aimed at parameterization of the breaking process to provide an approximate energy dissipation rate during wave breaking at coastlines with very gentle or mild bottom slopes (Battjes and Janssen, 1979; Thornton and Guza, 1983; Dally et al., 1985; Lippmann et al., 1996 and many others). All these models try to make accurate surf zone predictions under the assumption that the bottom profile and some offshore wave parameters are known. Since the details of the breaking process are still poorly understood, the models require the specification of some free unconstrained coefficients. For steep reef slopes the situation is even worse. At present, except some experimental estimations (Gerritsen, 1981; Gourlay, 1994; Hardy and Young, 1996; Hardy et al., 1991), there are no well documented parameterizations of the breaking process at steep slopes.

To develop a parameterization of breaking at steep bottom slopes, existing models for gentle slopes have been examined in terms of their applicability for steeper bottom slopes. After many preliminary tests, the periodic bore model of Battjes and Janssen (1979) was selected for further modification and adaptation. In this model, the rate of energy dissipation per unit area for each bore in a periodic wave train inside the surf zone is given by (see also Massel and Belberova, 1990; Dingemans, 1997):

$$\langle \epsilon_b \rangle = \frac{\alpha \rho g \omega}{8\pi} \frac{\sqrt{gh}}{C} \frac{H^3}{h}, \quad (26)$$

in which α is a free empirical coefficient which will be discussed in Section 2.5. Substitution of Eq. (26) into Eq. (24) gives a final expression for the damping factor γ_b :

$$\gamma_b = \frac{\alpha \omega}{\pi} \frac{\sqrt{gh}}{CC_g} \frac{H}{h}. \quad (27)$$

The initiation of energy dissipation or the extent of the surf zone, in which Eq. (27) should be used, is controlled by the non-dimensional maximum allowable wave height (H_m/h). As the reef-face bottom slope is much steeper than the slope of the reef-top, two different forms of (H_m/h) have been used, depending on a local reef slope. (a) On a reef-face when $|dh/dx| > 0.025$ (Singamsetti and Wind, 1980):

$$\frac{H_m}{h} = 0.937 \left| \frac{dh}{dx} \right|^{0.155} \left(\frac{H_0}{L_0} \right)^{-0.130}, \quad (28)$$

where H_0 and L_0 are deepwater wave height and length, respectively. (b) On a reef-top when $|dh/dx| < 0.025$ (Massel, 1996b):

$$\frac{H_m}{h} = \left[\frac{\sqrt{1 + 0.01504 h_*^{-2.5}} - 1}{0.1654 h_*^{-1.25}} \right]^2, \quad (29)$$

where:

$$h_* = \frac{h}{gT^2}. \quad (30)$$

In fact, formula (29) is a different representation of the formula proposed by Nelson (1994) in terms of the so-called non-linearity parameter F_c , originally developed by Swart and Loubser (1979):

$$F_c = \left(\frac{H}{h} \right)^{1/2} \left(T \sqrt{\frac{g}{h}} \right)^{5/2}. \quad (31)$$

2.4. Energy dissipation due to bottom friction

At a sandy coastline, energy dissipation due to bottom friction is much smaller than dissipation due to wave breaking. However, at reef slopes colonized by various types of corals, the bottom roughness can be very high. Let us start with the common expression for the average rate of energy dissipation in waves due to bottom friction (Gerritsen, 1981):

$$\langle \epsilon_f \rangle = \frac{2}{3\pi} \rho f_r |u_b|^3, \quad (32)$$

in which the friction coefficient f_r has now a value from 0.1 to 0.2 in natural conditions (Nelson, 1996). For a steep bottom slope, the bottom velocity u_b changes rapidly; thus the changes of a local wave number should be taken into account as well, i.e.:

$$\begin{aligned} u_b &= \frac{\partial \Phi_2}{\partial x} \Big|_{z=-h} = \frac{-igH_1}{2\omega} \exp(i\chi y) \exp(-\omega t) \frac{\cosh k_2(z+h_2)}{\cosh k_2 h_2} \\ &\times \left\{ \frac{\partial \varphi(x)}{\partial x} + \varphi(x) \left[\tanh k_2(z+h_2) \frac{d[k_2(z+h_2)]}{dx} \right. \right. \\ &\quad \left. \left. - \tanh(k_2 h_2) \frac{d(k_2 h_2)}{dx} \right] \right\} \Big|_{z=-h} \\ &= \frac{-igH_1}{2\omega} \exp(-i\omega t) \frac{\exp(i\chi y)}{\cosh(k_2 h_2)} \left\{ \frac{\partial \varphi(x)}{\partial x} - \varphi(x) \tanh(k_2 h_2) \frac{k_2}{2} \right. \\ &\quad \left. \times \left(\frac{C}{C_g} \right) \frac{dh_2(x)}{dx} \right\} \end{aligned} \quad (33)$$

After substitution of Eq. (32) into Eq. (25), a damping factor due to bottom friction is obtained as:

$$\gamma_f = \frac{16 f_r}{3\pi} \frac{|u_b|^3}{g C_g H^2}, \quad (34)$$

in which wave height H is given by Eq. (18).

2.5. Determination of empirical coefficient α

In Eq. (27) the only unknown quantity is the coefficient α . This coefficient describes the deviation of actual breaking from the periodic bore form. Numerous tests for gentle

slopes (Battjes and Janssen, 1979; Thornton and Guza, 1983; Massel, 1996a) have shown that this coefficient should be of $O(1)$. However, the value of α is totally unknown for steep slopes and for a fully predictive model it is desirable to define the coefficient α as a function of quantities which are already known. In this paper an attempt has been made to link the coefficient α with Swart and Loubser's type parameter F_c (Eq. (31)). Nelson (1994) has used F_c , based on local values of H and h , in an analysis of field data for wave transformation on a reef. Using laboratory experimental data Gourlay (1994) has argued that F_c , when based on deepwater wave height H_0 and a representative depth over the reef h_r , is a suitable parameter for classifying wave transformation on a coral reef. Because of involvement of deepwater wave height H_0 , we denote F_c by F_{c0} , i.e.:

$$F_{c0} = \left(\frac{H_0}{h_r} \right)^{1/2} \left(T \sqrt{\frac{g}{h_r}} \right)^{5/2}. \quad (35)$$

In order to accommodate various reef-rim geometries, a representative water depth h_r may be defined as the still water depth over the reef-edge, or as the average still water depth over the reef-rim between the reef-edge and reef-crest, or as the average still water depth over the reef-rim between the break point and the reef-crest (Gourlay, 1996b).

Unfortunately, the parameter F_{c0} does not contain any information on the reef-face slope β . To take into account the dependence of α also on the reef bottom slope we assume a relationship between α and reef geometry and incident wave parameters in a more general form as:

$$\alpha = f(F_{c0}, \beta), \quad (36)$$

in which β is a representative slope of the reef-face. The preliminary tests showed that, for convenience of further analysis, the following form of relationship (36) will be useful:

$$\alpha = 0 \text{ if } F_{c0} \leq F_{c0}^{(\text{lim})}$$

$$\alpha = a(F_{c0} - F_{c0}^{(\text{lim})})^b \text{ if } F_{c0} > F_{c0}^{(\text{lim})},$$

where $F_{c0}^{(\text{lim})}$ is a threshold value of parameter F_{c0} at which observed (or calculated) values of energy dissipation and set-up are negligible small. The practical implementations of formula (37) for various reef profiles are discussed in Section 3.

3. Application of the model for specific sites

3.1. Introduction

Laboratory experiments on waves propagating over coral reefs are not numerous. A summary of the results of these experiments has been presented by Gourlay (1996b) and will be not given here. We only note that the reef profiles used in experiments represent a wide range of reef types and profile shapes. Half the prototype reefs are fringing reefs,

half of them are platform reefs. Geographically half of them are in the Great Barrier Reef off northeastern Australia, the others are on islands in the Pacific and Indian Oceans. More details on reef geometry and laboratory models can be found in various papers by Gourlay (1994; 1996a; b).

3.2. Hayman Island reef

Hayman Island is a continental island in North Queensland (Australia). The typical reef profile adopted for the experiments is shown in Figs. 2 and 3. The reef-face with a slope of 1 to 4.5 rises from a depth of 19 or 21 m, while the water depth at reef-edge varies from 3.1 to 5.1 m depending on the tide level. The reef-top is initially sloping but the slope reduces away from the edge until the reef-top becomes horizontal 170 m from the reef-edge. The total reef width is of the order of 800 m. It should be noted that in the Hayman Island laboratory model, the incident “ocean” water depth has been reduced to

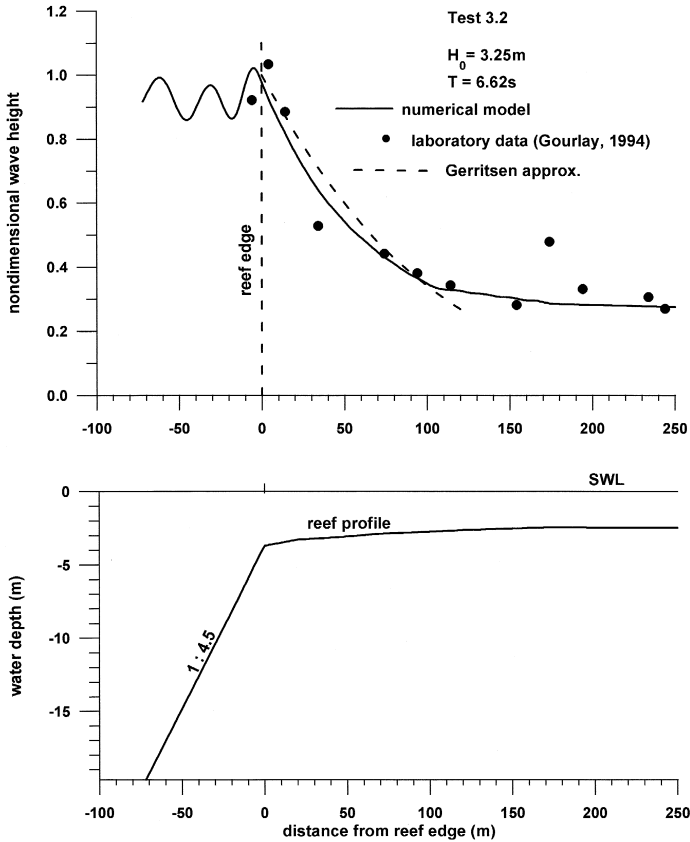


Fig. 2. Comparison of theoretical and experimental wave height attenuation over Hayman Island reef for high incident wave.

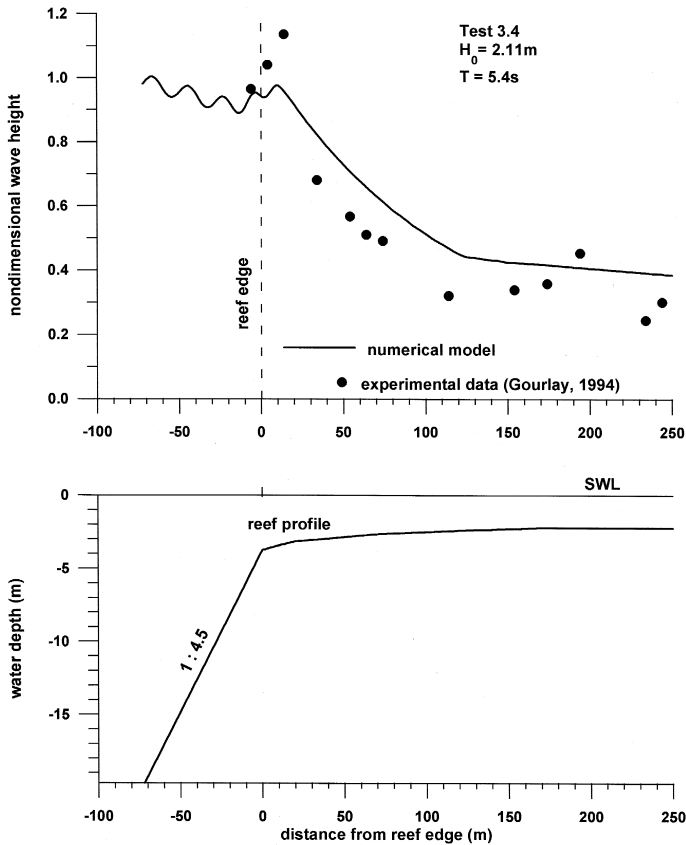


Fig. 3. Comparison of theoretical and experimental wave height attenuation over Hayman Island reef for smaller incident wave.

8 m. However, the influence of this reduction on wave transformation and wave-induced set-up was negligible small and all calculations have been done for the prototype reef profile.

The incident deepwater wave height used in experiments varies from 1.02 to 3.61 m and the wave period is in a range from 3.8 to 6.8 s. Three water levels were chosen for experiments corresponding to highest astronomical tide (HAT), mean high water neap (MHWN) and MSL. In each case, 0.3 m was added to allow for storm surge. In the paper of Gourlay (1994), all experimental values were presented in prototype units, having been scaled using Froude similarity law assuming that gravity forces predominate. Wave heights were measured at locations determined by visually observed changes in wave conditions, usually at a dozen or so locations. Wave set-up was measured by piezometers spaced at 60 m (prototype) intervals.

At Hayman Island reef (mean reef-face slope $\sim 1:4.5$), waves initially plunge on the reef-edge and dissipate almost all their energy within five wavelengths of the reef-edge

when $160 < F_{c0} < 530$. When $100 < F_{c0} < 150$, waves spill on the outer reef-top and when $70 < F_{c0} < 100$, waves spill further inshore on the reef-top. For smaller values of F_{c0} waves either just break on the horizontal reef-top or pass over it without breaking. To find the dependence of the unknown coefficient α on F_{c0} for a given reef-face slope, the following sub-set of experimental data on wave height transformation and wave-induced set-up for Hayman Island reef was used: runs 1.1, 1.3, 2.3, 2.4, 2.5 and 3.3 (run numbers are the same as in Gourlay, 1994). This calibration, based on the minimalization of the least square error between predicted and experimental values results in the following relationship for α :

$$\alpha = 0 \text{ if } F_{c0} \leq 100$$

$$\alpha = 0.0156(F_{c0} - 100)^{0.576} \text{ if } F_{c0} > 100. \quad (38)$$

Thus, using the form Eq. (37), we find that for $\beta = 1/4.5$, the parameters a , b and F_{c0}^{lim} are 0.0156, 0.576 and 100, respectively. When $F_{c0} < 100$, there is no reduction of wave energy due to breaking, but some energy still can be dissipated by bottom friction.

Now, we are in position to determine the wave height variation and wave-induced set-up across the reef in a fully predictable way. Firstly, the coefficient α is calculated from Eq. (38) for known incident wave parameters. Then, Eqs. (11) and (22) are solved simultaneously in an interactive manner. Next, using the potentials Φ_1 , Φ_2 and Φ_3 , given by Eqs. (1), (9) and (5), the variations of wave height in all Regions are obtained, i.e.:

$$\text{Region I: } H(x, y) = H_i |\exp(ik_1 x \cos \theta_1) + K_R \exp(-ik_1 x \cos \theta_1)| \exp(i\chi y), \quad (39)$$

$$\text{Region II: } H(x, y) = H_i |\varphi(x) \exp(i\chi y)|, \quad (40)$$

$$\text{Region III: } H(x, y) = |K_T \exp[ik_3(x - b) \cos \Theta_3]| \exp(i\chi y). \quad (41)$$

In Fig. 2 an example of attenuation of non-dimensional wave height ($H(x)/H_0$) over a distance of 250 m from the reef-edge for $F_{c0} = 620$ is shown. Agreement between numerical and experimental results is very good. The oscillation in wave height at the front of the reef is caused by partial reflection of waves from the reef structure. Waves are plunging on the reef-edge and dissipate almost all their energy within 100 m of the reef-edge. The reflection coefficient is very small, $K_r = 6.7\%$ and the transmission coefficient $K_t = 29.1\%$. This means that about 95% of wave energy is dissipated by wave breaking.

For comparison in the same figure a simplified analytical solution, developed by Gerritsen (1981), is shown. On the reef-top where $h(x) \approx \text{const}$ and bottom friction can be neglected, a decaying of wave height is given by (Gerritsen, 1981):

$$H(x) = H(0) \exp\left(-\frac{B}{A}\right), \quad (42)$$

in which $H(0)$ is the reference wave height at a reef-edge, x is the distance from reef-edge and the coefficients A and B are:

$$A = \frac{1}{4} \rho g C_g \approx \frac{1}{4} \rho g C \quad (43)$$

$$B = \frac{\xi \rho g}{4\sqrt{2} T}. \quad (44)$$

Coefficient ξ is of an order one and is given by (Gerritsen, 1981):

$$\xi = \frac{\alpha H_* \sqrt{2 + H_*}}{Fr \sqrt{1 + H_*}} \quad (45)$$

in which:

$$Fr = \frac{C}{\sqrt{gh(x)}} \text{ and } H_* = \frac{H(x)}{h(x)}. \quad (46)$$

Attenuation of wave height in Fig. 2 was given for $\xi = 0.5$. It should be noted that approximation (42) is valid for a distance $0 < x < 120$ m where wave breaking dominates the bottom friction.

The case when smaller waves are plunging on the outer reef-top (F_{c0} is smaller than 300) is demonstrated in Fig. 3. The attenuation of wave height is more gentle than in Fig. 2 with reflection coefficient $K_r = 2.7\%$, transmission coefficient $K_t = 39.1\%$ and the percentage of dissipated energy is equal to 85%.

The values of reflection and transmission coefficients K_R and K_T , are shown in Fig. 4. Definition of reflection and transmission coefficients follows directly from Eqs. (1) and (5). It should be noted that this definition is different than the experimental

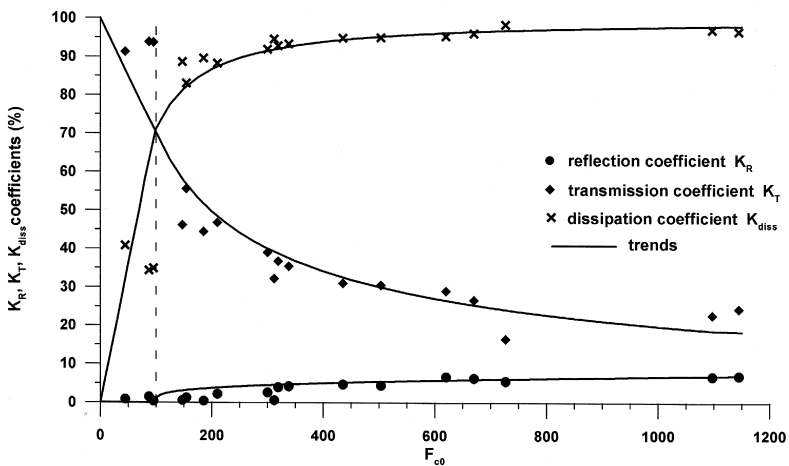


Fig. 4. Reflection, transmission and dissipation coefficients as a function of F_{c0} .

technique (antinodal nodal pattern analysis) used by Gourlay (1994). Therefore, no attempt has been made to compare the calculated and experimental coefficients.

In all cases reflection from the reef-face, while increasing slowly, remains small for all F_{c0} values. The transmission coefficient K_T attenuates as F_{c0} increases and the rate of attenuation of wave energy is controlled by wave breaking and bottom friction. In calculations friction coefficient $f_r = 0.01$ was used since it is believed that the laboratory model reef surface was smoother than natural reef surfaces.

Additionally, in Fig. 4 the dissipation coefficient K_{diss} is shown. This coefficient can be determined from the balance of the reflected, transmitted and dissipated wave energy as follows:

$$K_{diss} = \left(\frac{E_{diss}}{E_i} \right)^{1/2} = \sqrt{1 - (K_R^2 + K_T^2)}, \tag{47}$$

in which E_{diss} and E_i are the dissipated and incident wave energy, respectively. For

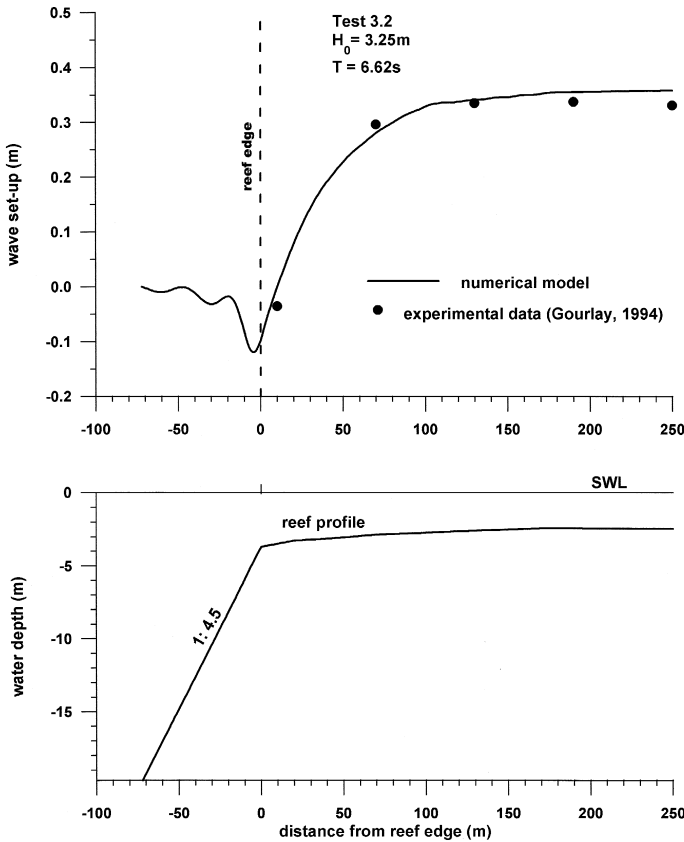


Fig. 5. Comparison of theoretical and experimental set-up value over Hayman Island reef for high incident wave.

$F_{c0} < 100$, the only dissipation mechanism is bottom friction and therefore the dissipation coefficient becomes much smaller than for higher F_{c0} values.

The set-up $\bar{\eta}$ induced by breaking waves is determined simultaneously with the transformation of waves on the reef profile. In Figs. 5 and 6 examples of set-up variation across the reef-top, corresponding to the wave conditions shown in Figs. 2 and 3, are given. As expected, the numerical model predicts small, negative set-up in the vicinity of wave breaking and rising water level on the reef-top. The agreement between the calculated and experimental set-up is very good.

The most important set-up characteristic is the maximum set-up $\bar{\eta}_{\max}$. This value is a significant factor in determining flooding and erosion of reef-protected coasts and flushing of reefal lagoons. In general, $\bar{\eta}_{\max}$ is a function of reef geometry and incident wave parameters. In particular, Gerritsen (1981) related the dimensionless set-up $\bar{\eta}/H_0$ to a modified Ursell parameter for shallow water (gT^2H_0/h_0^2). In fact, this representation is equivalent to the relationship between $\bar{\eta}_{\max}/H_0$ and two dimensionless quantities,

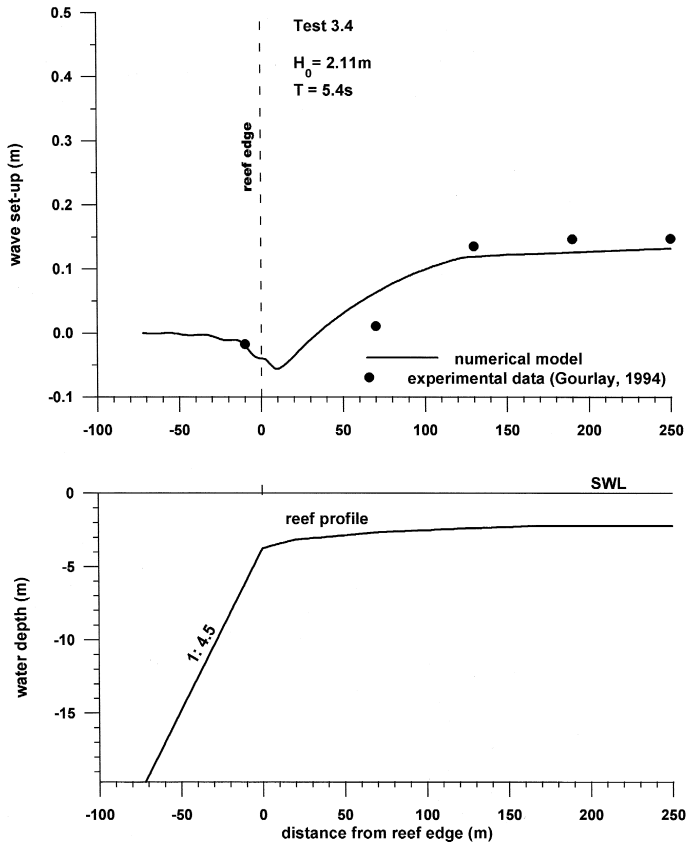


Fig. 6. Comparison of theoretical and experimental set-up over Hayman Island reef for smaller incident wave.

i.e., relative reef depth (h_3/H_0) and incident wave steepness (H_0/gT^2). However, in order to provide a comparison between calculated values and measured data, the dimensionless parameters $\bar{\eta}_{\max}/T\sqrt{gH_0}$ and $(\bar{\eta}_{\max} + h_3)/H_0$ introduced by Gourlay (1996b; 1997) will be used. The results of comparison are presented in Fig. 7. The tendencies in both, calculated and experimental values, are the same. Gourlay (1996b), using a theoretical analysis of energy fluxes and his experimental data, showed that a relationship between $\bar{\eta}_{\max}/T\sqrt{gH_0}$ and $(\bar{\eta}_{\max} + h_3)/H_0$ takes the form:

$$\frac{\bar{\eta}_{\max}}{T\sqrt{gH_0}} = \frac{3}{64\pi} K_p \left[(1 - K_R^2) - 4\pi\gamma_r^2 \left(\frac{\bar{\eta}_{\max} + h_3}{H_0} \right)^2 \frac{1}{T} \sqrt{\frac{\bar{\eta}_{\max} + h_3}{g}} \right] \times \left(\frac{H_0}{\bar{\eta}_{\max} + h_3} \right)^{3/2}, \tag{48}$$

in which K_p is a reef profile shape factor representing the difference between observed and predicted set-up, and γ_r is a reef-top breaker index. If we assume $K_p = 0.44$, $K_R = 0$, $\gamma_r = 0.4$ and $T\sqrt{g}/(\bar{\eta}_{\max} + h_3) = 15$, as suggested by Gourlay (1996b), we obtain:

$$\frac{\bar{\eta}_{\max}}{T\sqrt{gH_0}} = 0.006565 \left[1 - 0.134 \left(\frac{\bar{\eta}_{\max} + h_3}{H_0} \right)^2 \right] \left(\frac{H_0}{\bar{\eta}_{\max} + h_3} \right)^{3/2}, \tag{49}$$

Relationship (49) is shown in Fig. 7. The agreement of this relationship with the

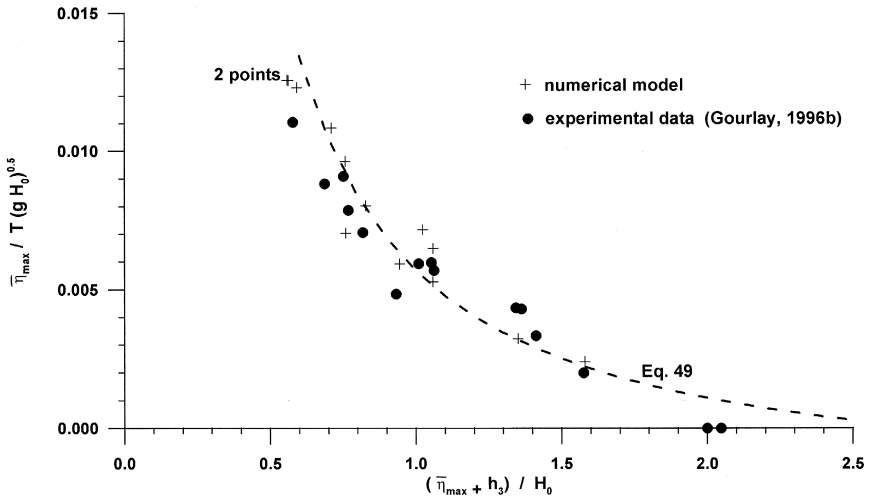


Fig. 7. Non-dimensional maximum set-up as a function of non-dimensional submergence for Hayman Island reef.

numerical model is very good, and for lower values of $(\bar{\eta}_{\max} + h_3)/H_0$ the agreement with numerical values is even better than with the experimental ones.

Let us rewrite Eq. (48) in a slightly different form:

$$\frac{\bar{\eta}_{\max}}{H_0} = \frac{3}{64\pi} K_p \left[(1 - K_R^2) - 4\pi\gamma_r^2 \left(\frac{H_0}{\bar{\eta}_{\max} + h_3} \right)^{3/2} U_0^{-1/2} \right] \left(\frac{H_0}{\bar{\eta}_{\max} + h_3} \right)^{1/2} U_0^{1/2}, \tag{50}$$

in which:

$$U_0 = \frac{gT^2 H_0}{(\bar{\eta}_{\max} + h_3)^2} = \frac{gT^2}{H_0} \left(\frac{H_0}{\bar{\eta}_{\max} + h_3} \right)^2 \tag{51}$$

is the shallow water form of the Ursell number expressed in terms of deepwater wave height and total depth on reef-top $(\bar{\eta}_{\max} + h_3)$.

Eq. (50) predicts that the maximum set-up is a function of both the Ursell number U_0 for shallow water and the inverse submergence $H_0/(\bar{\eta}_{\max} + h_3)$ to power 1/2. However, the proportionality coefficients (terms in brackets) are also functions of a priori unknown $\bar{\eta}_{\max}$ and U_0 . In other words, Eq. (50) is a transcendental equation for $\bar{\eta}_{\max}$ and can only be solved in an iterative manner as shown by Gourlay (1997).

In this paper, as was explained in Section 2, $\bar{\eta}_{\max}$ values are solved simultaneously with the wave height H values in one numerical scheme. In Fig. 8, resulting numerical as well as experimental values of $\bar{\eta}_{\max}/H_0$ are shown as a function of the Ursell number U_0 . The numerical values agree well with experiments.

For this set of experiments the values of gT^2/H_0 are approximately constant. Hence, scatter of both experimental and numerical points reflect variations in $H_0/(\bar{\eta}_{\max} + h_3)$.

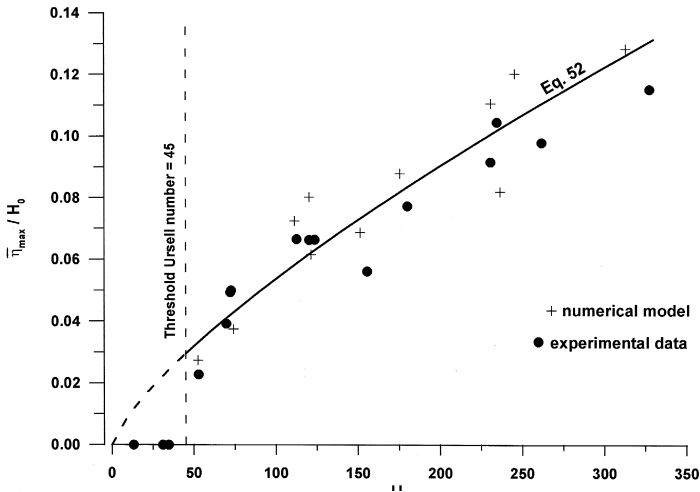


Fig. 8. Non-dimensional maximum set-up as a function of the Ursell number for Hayman Island reef.

The values of $\bar{\eta}_{\max}/H_0$ increase monotonically with Ursell number and this trend can be represented approximately by the following equation:

$$\frac{\bar{\eta}_{\max}}{H_0} = 0 \text{ for } U_0 \leq U_{c0} = 45$$

$$\frac{\bar{\eta}_{\max}}{H_0} = 0.0017U_0^{0.75} \text{ for } U_0 > U_{c0}, \tag{52}$$

also shown in Fig. 8. However, this relationship is valid for Ursell numbers greater than about 45. Below this threshold value, set-up is negligibly small. A similar threshold value results also from Eq. (50), in which the first bracket becomes zero at about $U_0 = 45$.

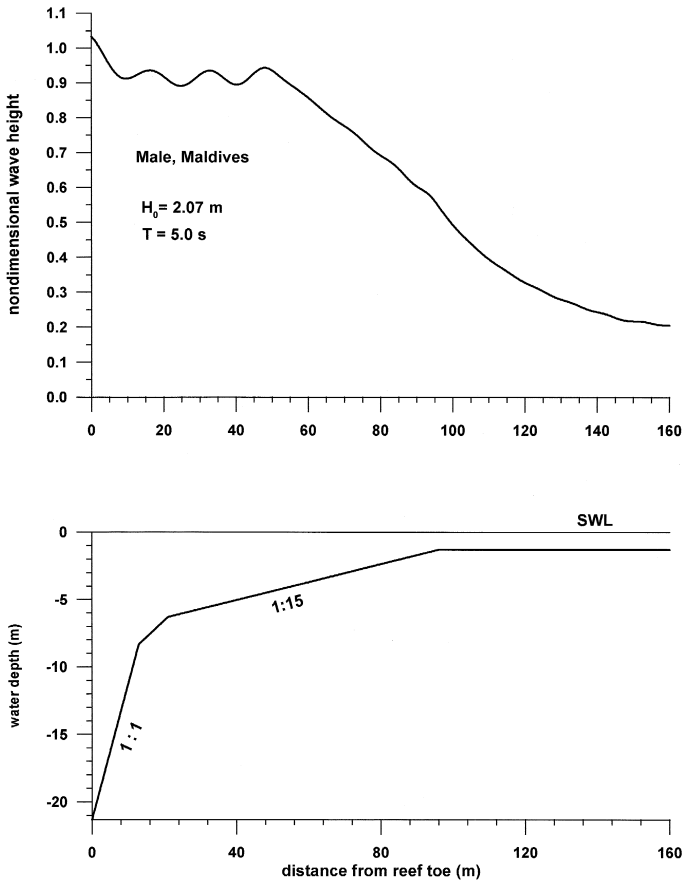


Fig. 9. Wave height attenuation over the Malé reef. Numerical result.

3.3. Malé Island reef

Jensen (1991) used laboratory experiments to investigate wave transformation and set-up on the reef at the southwestern corner of the island of Malé in the Maldives (Indian Ocean) in connection with the development of a new harbour for this part of the reef. The reef is characterized by a very steep slope of about 1:1 from water depth 21.3 m till a water depth of 8.3 m. Between water depths of 8.3 and 6.3 m, a slope of 1:4 was used, while for depths smaller than 6.3 m the average slope is 1:15 up to reef-crest. Water depth at reef-top was assumed to be constant and equal to 1.3 m.

The laboratory tests have been performed for three wave periods, i.e., $T = 5, 10$ and 15 s and for four different wave heights for each wave period. The measured quantities include mean set-up and its standard deviation, maximum wave crest elevation and wavefront velocities.

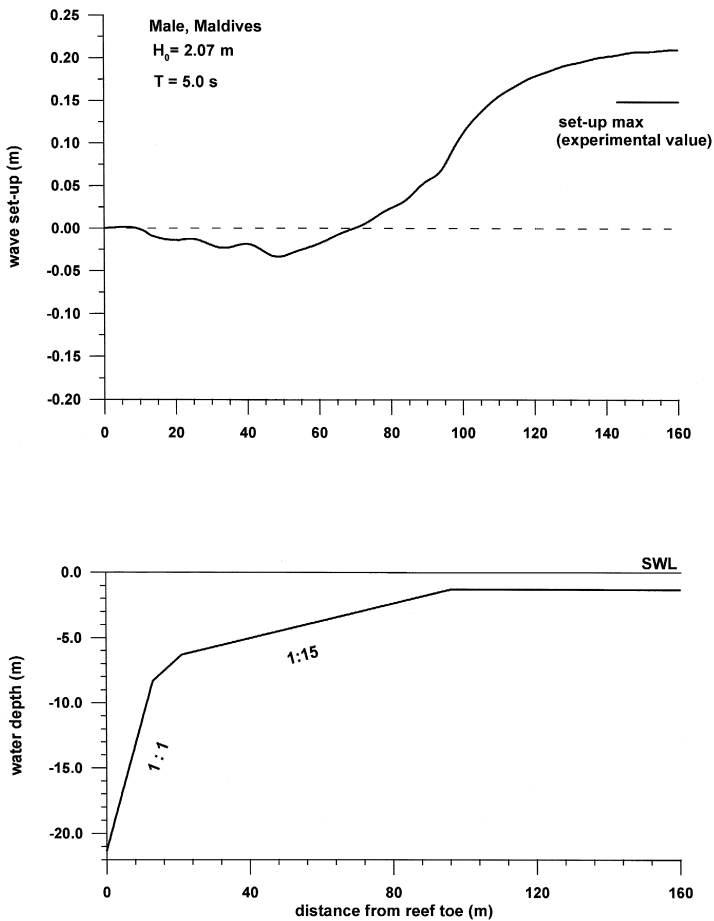


Fig. 10. Set-up over the Malé reef. Numerical result.

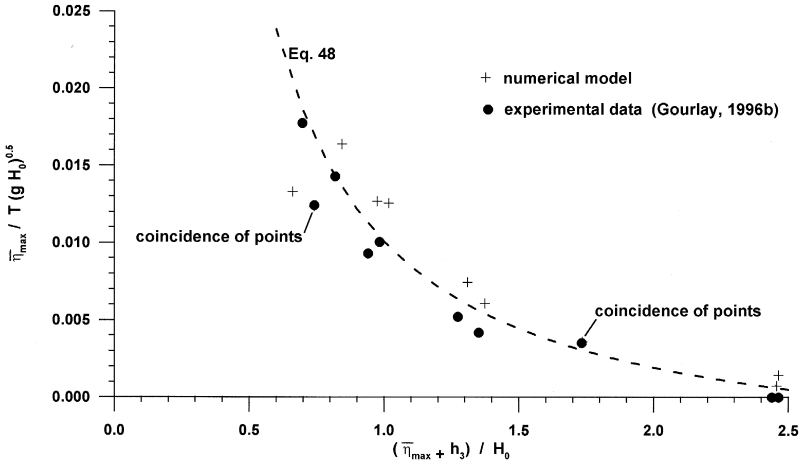


Fig. 11. Non-dimensional maximum set-up as a function of non-dimensional submergence for the idealized reef.

The relationship $\alpha = f(F_{c0}, \beta)$ for runs with wave periods 5 and 10 s, which provides the best approximation for observed maximum set-up values, fits very well into the general formula (37) with the following parameters: $a = 0.0208$, $b = 0.560$ and $F_{c0}^{(lim)} = 100$, i.e.,

$$\alpha = 0 \text{ if } F_{c0} \leq 100$$

$$\alpha = 0.0208(F_{c0} - 100)^{0.56} \text{ if } F_{c0} > 100. \tag{53}$$

Figs. 9 and 10 give an example of calculated wave height and set-up over the reef profile. Initially, wave height drops at the reef-face. Then, owing to the relatively long

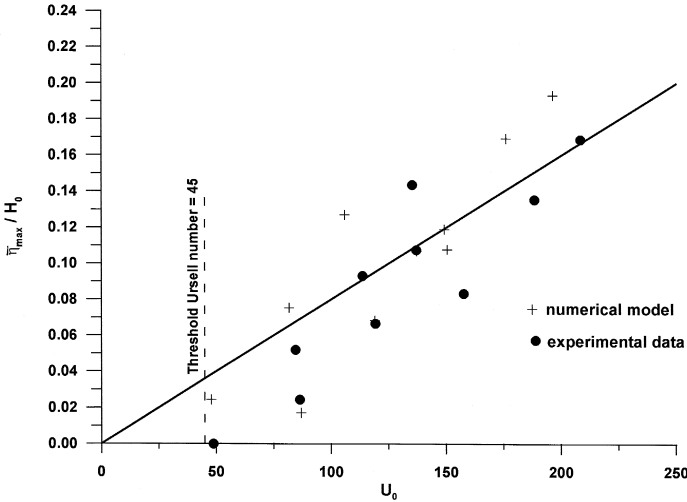


Fig. 12. Non-dimensional maximum set-up as a function of the Ursell number for the idealized reef.

gradually shoaling reef-rim, wave height oscillates before final breaking over the reef slope in front of the reef.

The oscillating wave height (also radiation stress) over the shoaling reef-rim induces a small lowering of the mean water level. Only when wave breaking commences, does set-up occur (see Fig. 10).

3.4. Idealized two-dimensional horizontal reef

Model arrangements and experimental results for wave transformation at an idealized two-dimensional reef model have been described by Gourlay (1996a). Therefore, only the basic model features are outlined here. A 400-mm high horizontal model reef with a particularly absorbent 1 to 1 face slope has been constructed. The sea bottom in front of the reef has a slope 1 in 84 and the effective reef height is 320 mm. The width of reef-top is about 15 m. Two wave periods of 1.48 and 1.10 s have been used and deepwater wave height varied from 41 to 218 mm. In the numerical model, only the runs

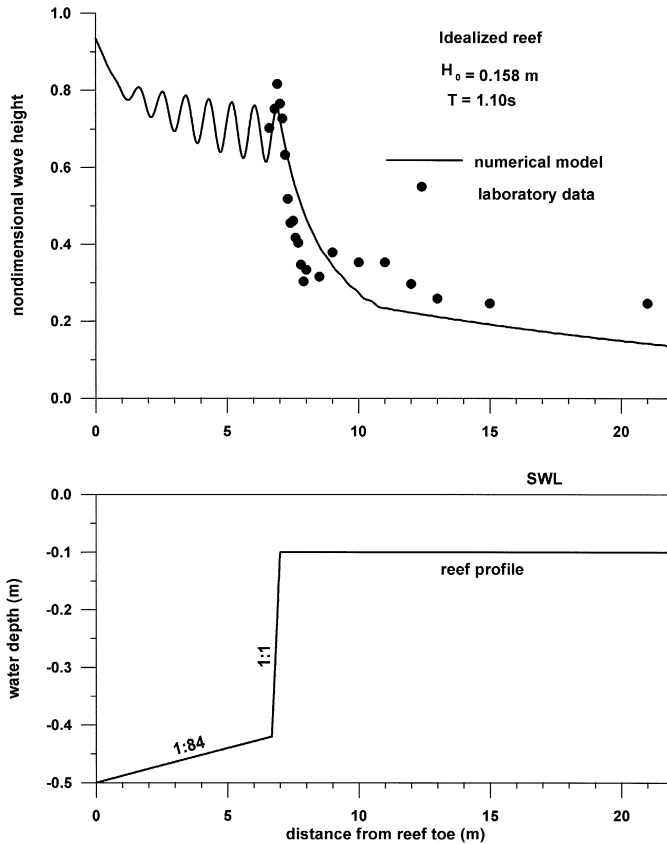


Fig. 13. Comparison of theoretical and experimental wave height attenuation over the idealized reef.

with 0.1 m water depth over the reef-top have been reproduced. Hence, the corresponding F_{c0} parameter ranges from 250 to 1214. The values of F_{c0} greater than about 1000 correspond to very shallow water, where the extended refraction–diffraction Eq. (11) is not applicable. Therefore, the following analysis has been restricted to runs when $F_{c0} < 1000$.

The calculations showed that the best agreement with experiments, in terms of the maximum set-up on the reef-top, was obtained with coefficient α satisfying the following relationship:

$$\alpha = 0 \text{ if } F_{c0} \leq 100$$

$$\alpha = 0.0252(F_{c0} - 100)^{0.517} \text{ if } F_{c0} > 100. \tag{54}$$

The relationships (53) and (54) are very similar, which is not surprising since both reefs have the similar reef-face slopes, namely 1 in 1.

In Fig. 11, non-dimensional maximum set-up $\bar{\eta}_{\max}/T\sqrt{gH_0}$ is shown as a function of non-dimensional submergence $(\bar{\eta}_{\max} + h_3)/H_0$. Numerical and experimental points ex-

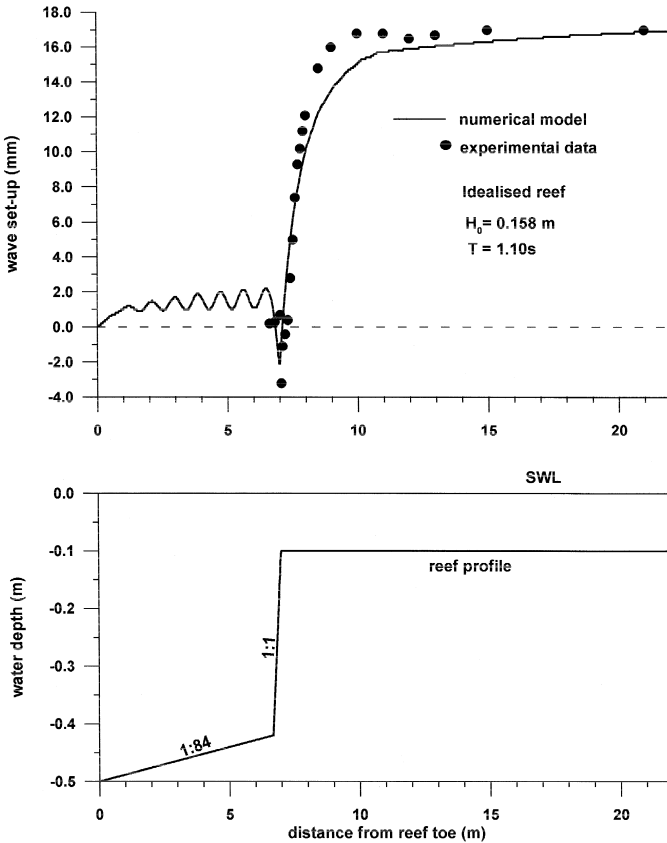


Fig. 14. Comparison of theoretical and experimental set-up value over the idealized reef.

hibit the same definable tendency and there is a close correspondence between both values (two points coincide exactly). In the same figure the relationship (48) suggested by Gourlay (1996b) is given with $K_p = 0.78$, $K_R = 0$, $\gamma_r = 0.4$ and $T\sqrt{g/(\bar{\eta}_{\max} + h_3)} = 15$. A comparison of Figs. 7 and 11 indicates that reef with steeper front face produces a higher set-up on a reef-top for the same submergence parameter values.

A dependence of the non-dimensional maximum set-up (experimental and numerical) on the Ursell number is illustrated in Fig. 12. The solid line gives the best linear fitting to the numerical and experimental data, and a corresponding equation of the straight line is:

$$\frac{\bar{\eta}_{\max}}{H_0} = 0.0008U_0. \quad (55)$$

A different power of the Ursell number U_0 illustrates an influence of the front reef slope on the maximum set-up value, and scatter of both experimental and numerical points reflect variations in $H_0/(\bar{\eta}_{\max} + h_3)$.

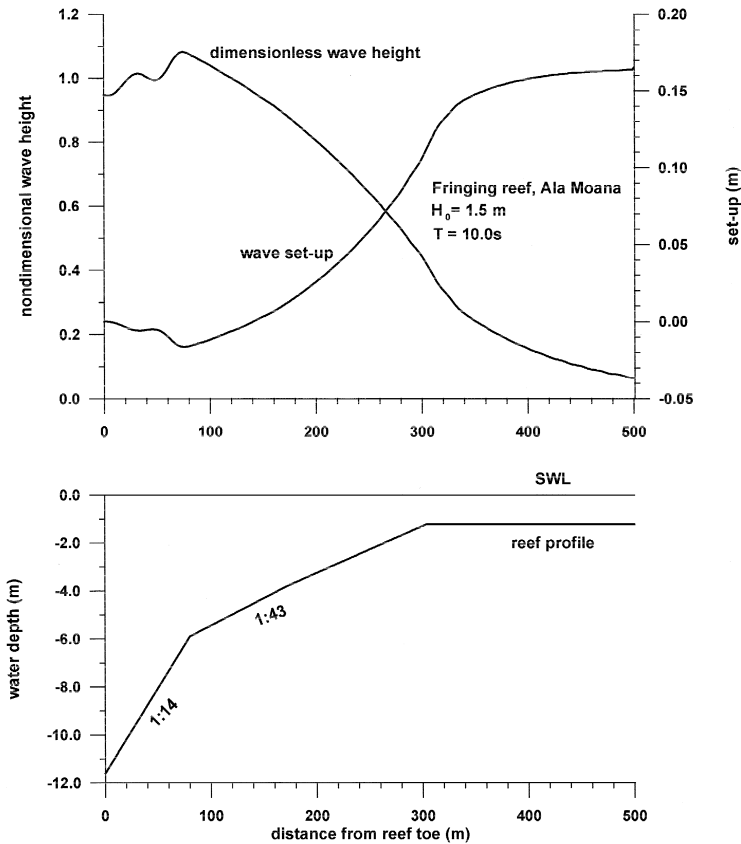


Fig. 15. Wave height attenuation and wave-induced set-up for Ala Moana Reef, HI. Numerical result.

An example of wave transformation on the idealized reef is shown in Fig. 13. The numerical calculations start at the fore reef slope and energy dissipation due to bottom friction and beginning of breaking increases. As a result, wave height decreases over a front slope of the reef and over the reef-top. The observed oscillations in wave height are a result of the partial reflection of the approaching waves.

Fig. 14 illustrates the corresponding set-up on the reef-top. Because wave height continually decreases, set-down only occurs on the reef-faces, and set-up gradually increases up to its maximum value that is reached at 3 m from reef-edge. At larger distances from the reef-edge, wave height remains almost constant and the set-up also does not change. The oscillations in set-up result from the oscillations of wave height (and radiation stress) at the reef front.

3.5. Fringing reef, Ala Moana Reef, HI

Gerritsen (1981) conducted comprehensive field and laboratory studies of wave attenuation and wave set-up along a transverse section of Ala Moana Reef at Honolulu.

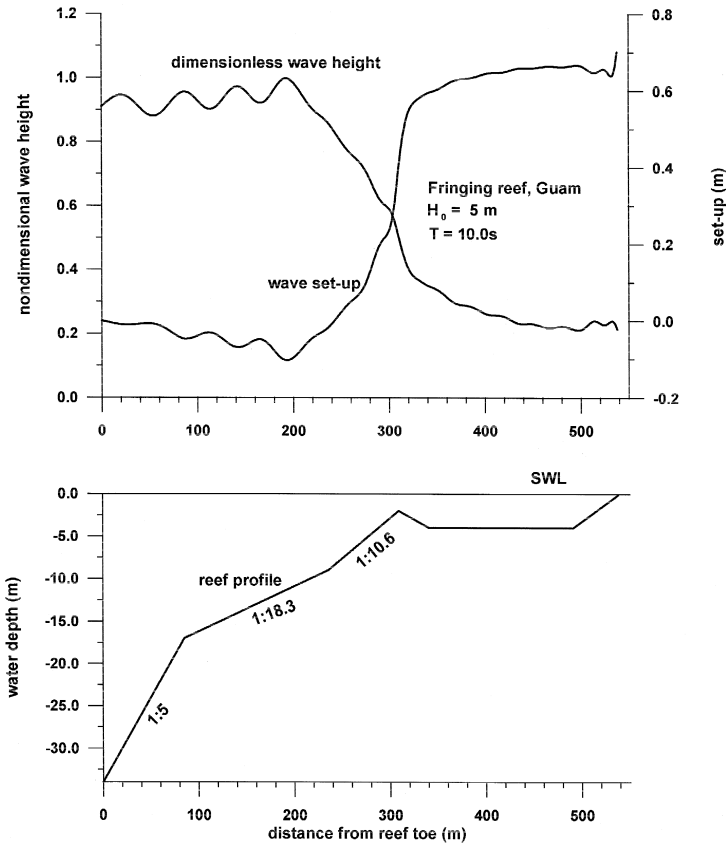


Fig. 16. Wave height attenuation and wave-induced set-up for fringing reef at Guam. Numerical result.

The application of the developed numerical model is demonstrated for a case of regular waves of incident height $H_0 = 1.5$ m and period of $T = 10$ s. Water depth on the reef-top of 1.22 m was assumed. The results of the calculations are given in Fig. 15. The very long incident wave, in comparison with water depth, gradually decays as it travels over the reef. Wave set-up is relatively small; the maximum value reaches about 16 cm. This value agrees very well with experimental values presented, for example, in summary Figs. 3 and 4 given by Gourlay (1996b).

3.6. Fringing reef at Guam

Seelig (1983) conducted laboratory experiments to investigate the influence of wind waves on set-up level and transmitted wave characteristics of an idealized reef–lagoon system. The laboratory study was designed to reproduce an expected design water level for the island of Guam. For the purpose of this study a case of regular waves incident on the reef with lagoon width of 150 m was chosen. As Seelig found, the lagoon width has little influence on the set-up for the range he tested. Incident wave parameters adopted in the numerical model are the following: $H_0 = 5.0$ m and $T = 10$ s. The water depth over the reef-crest is 2 m. The variations of non-dimensional wave height and set-up across the reef and lagoon are given in Fig. 16. As the waves are rather high, they start to break offshore of reef-crest and subsequently decay when moving inshore. Set-up rapidly rises in front of the reef-crest but then changes only marginally over the reef lagoon. Close to the shoreline set-up increases again due to the breaking of reformed waves. The mean value of set-up in the reef lagoon (about 64 cm) is a little lower than the equivalent value of 80 cm derived from Seelig's experimental data (see Gourlay, 1996b; Figs. 3 and 4).

4. Conclusions

(1) In this paper, a numerical model, designed for prediction of wave transformation and wave-induced set-up, has been presented. This model is based on the extended refraction–diffraction equation (Massel, 1993) which allows relatively steep slopes and arbitrary bottom shapes.

(2) Reef slopes as steep as 1:1 can be modelled under the assumption that the dimensionless submergence $(\bar{\eta}_{\max} + h_3)/H_0$ is larger than ≈ 0.6 . Numerical modelling and experimental data have shown that set-up is negligible for the Ursell number $U_0 < 45$.

(3) Two energy dissipation mechanisms have been incorporated into this model, i.e., wave breaking and bottom friction. The wave breaking process has been parameterized using a modification of the Battjes and Janssen (1979) periodic bore approach. A free empirical coefficient α has been related to the incident wave parameters and the characteristic water depth at the reef through the dimensionless parameter F_{c0} . The experimental data (Gourlay, 1994, 1996a,b) has been used to calibrate the dependence of α on F_{c0} .

(4) For a known value of α , the proposed model can predict wave transformation and wave-induced set-up at all points across a reef. The applicability of the developed model

has been demonstrated for reefs of various shapes subjected to various incident wave conditions. Comparison of predicted and observed wave heights and set-up values showed good agreement. The model is easily implemented on the common PC computer and the time for calculations is of the order of seconds.

(5) Many natural reefs may vary in elevation in the y -direction. This variation induces a horizontal circulation which affects wave set-up. A paper on wave transformation and wave set-up, when flow over reef is permitted, is now under preparation.

References

- Battjes, J.A., Janssen, J.P.F.M., 1979. Energy loss and set-up due to breaking of random waves. Proc. 16th Coastal Eng. Conf., Hamburg, 1978, 1, 563–587.
- Berkhoff, J.C.W., 1973. Computation of combined refraction-diffraction. Proc. 13th Coastal Eng. Conf., Vancouver, 1972, 1, 471–490.
- Dally, W.R., Dean, R.G., Dalrymple, R.A., 1985. Wave height variation across beaches of arbitrary profiles. *J. Geophys. Res.* 90, 10917–10927.
- Dingemans, M.W., 1997. *Water Wave Propagation over Uneven Bottoms: Part 1. Linear Wave Propagation*. World Scientific, Singapore, 471 pp.
- Gerritsen, F., 1981. Wave attenuation and wave set-up on a coastal reef. Univ. Hawaii — Look Lab. Tech. Rep. No. 48, 416 pp.
- Gourlay, M.R., 1994. Wave transformation on a coral reef. *Coastal Eng.* 23, 17–42.
- Gourlay, M.R., 1996a. Wave set-up on coral reefs: 1. Set-up and wave-generated flow on an idealized two dimensional horizontal reef. *Coastal Eng.* 27, 161–193.
- Gourlay, M.R., 1996b. Wave set-up on coral reefs: 2. Set-up on coral reefs with various profiles. *Coastal Eng.* 28, 17–55.
- Gourlay, M.R., 1997. Wave set-up on coral reefs: some practical applications. Proc. Pacific Coasts and Ports, 1997, Christchurch, 2, 959–964.
- Haggerty, G.B., 1971. *Elementary Numerical Analysis with Programming*. Allyn and Bacon, Boston, 476 pp.
- Hardy, T.A., Young, I.R., 1996. Field study of wave attenuation on an offshore coral reef. *J. Geophys. Res.* 101, 14311–14326.
- Hardy, T.A., Young, I.R., Nelson, R.C., Gourlay, M.R., 1991. Wave attenuation on an offshore coral reef. Proc. 22nd Coastal Eng. Conf., Delft, 1990, 1, 330–344.
- Jensen, O., 1991. Waves on coral reefs. Proc. 7th Symp. Coastal and Ocean Management, Long Beach, 3, 2668–2680.
- Lee, T.T., Black, K.P., 1979. The energy spectra of surf waves on a coral reef. Proc. 16th Coastal Eng. Conf., Hamburg, 1978, 1, 588–608.
- Lippmann, T.C., Brookins, A.H., Thornton, E.B., 1996. Wave energy transformation on natural profiles. *Coastal Eng.* 27, 1–20.
- Longuet-Higgins, M.S., Stewart, R.W., 1964. Radiation stresses in water waves: a physical discussion with applications. *Deep Sea Res.* 11, 529–562.
- Massel, S.R., 1989. *Hydrodynamics of Coastal Zones*. Elsevier, Amsterdam, 336 pp.
- Massel, S.R., 1993. Extended refraction–diffraction equation for surface waves. *Coastal Eng.* 19, 97–126.
- Massel, S.R., 1994. Measurement and modelling of waves incident on steep islands or shoals. Proc. Int. Symp.: Waves Physics and Numerical Modelling, Vancouver, 2, 982–991.
- Massel, S.R., 1996a. *Ocean Surface Waves: Their Physics and Prediction*. World Scientific, Singapore, 491 pp.
- Massel, S.R., 1996b. On the largest wave height in water of constant depth. *Ocean Eng.* 23, 553–573.
- Massel, S.R., Belberova, D.Z., 1990. Parameterization of the dissipation mechanisms in the surface waves induced by wind. *Arch. Mech.* 42, 515–530.
- Massel, S.R., Brinkman, R.M., 1998. Measurement and modelling of wave propagation and breaking at steep reefs. In: Saxena, N. (Ed.), *Recent Advances in Marine Science and Technology*, 1998. Pacon Int., in press.

- Nelson, R.C., 1994. Depth limited design wave heights in very flat regions. *Coastal Eng.* 23, 43–59.
- Nelson, R.C., 1996. Hydraulic roughness of coral reef platforms. *Appl. Ocean Res.* 18, 265–274.
- Roberts, H.H., 1981. Physical processes and sediment flux through reef–lagoon systems. *Proc. 17th Coastal Eng. Conf., Sydney, 1980*, 1, 946–962.
- Seelig, W.N., 1983. Laboratory study of reef–lagoon system hydraulics. *J. Waterw., Port, Coastal, Ocean Eng.* 109, 380–391.
- Singamsetti, S.R., Wind, H.G., 1980. Breaking waves; characteristics of shoaling and breaking periodic waves normally incident to plane beaches of constant slope. *Delft Hydraulics, Rep. M1371*, 80 pp.
- Swart, D.H., Loubser, C.C., 1979. Viscoidal theory for full non-breaking waves. *Proc. 16th Coastal Eng. Conf., Hamburg, 1978*, 1, 467–486.
- Thornton, E.B., Guza, R.T., 1983. Transformation of wave height distribution. *J. Geophys. Res.* 88, 5925–5938.
- Veron, J.E.N., 1986. *Corals of Australia and the Indo-Pacific*. Univ. Hawaii Press, Honolulu, 644 pp.
- Young, I.R., 1989. Wave transformation over coral reefs. *J. Geophys. Res.* 94, 9779–9789.